

# SDSS J114657.79+403708.6: the third most distant blazar at $z=5.0$

G. Ghisellini<sup>1</sup>, \* T. Sbarrato<sup>1,2,3</sup>, G. Tagliaferri<sup>1</sup>, L. Foschini<sup>1</sup>, F. Tavecchio<sup>1</sup>, G. Ghirlanda<sup>1</sup>, V. Braitto<sup>1</sup>, N. Gehrels<sup>4</sup>

<sup>1</sup> INAF – Osservatorio Astronomico di Brera, via E. Bianchi 46, I-23807 Merate, Italy

<sup>2</sup> Univ. dell’Insubria, Dipartimento di Fisica e Matematica, Via Valleggio 11, I-22100 Como, Italy

<sup>3</sup> ESO–European Southern Observatory, Karl–Schwarzschild–Strasse 2, 8578 Garching bei München, Germany

<sup>4</sup> NASA–Goddard Space Flight Center, Greenbelt, Maryland 2077, USA

17 August 2021

## ABSTRACT

The radio–loud quasar SDSS J114657.79+403708.6 at a redshift  $z=5.0$  is one of the most distant radio–loud objects. The IR–optical luminosity and spectrum suggest that its black hole has a very large mass:  $M = (5 \pm 1) \times 10^9 M_\odot$ . The radio–loudness (ratio of the radio to optical flux) of the source is large (around 100), suggesting that the source is viewed at small angles from the jet axis, and could be a blazar. The X–ray observations fully confirm this hypothesis, due to the high level and hardness of the flux. This makes SDSS J114657.79+403708.6 the third most distant blazar known, after Q0906+693 ( $z = 5.47$ ) and B2 1023+25 ( $z = 5.3$ ). Among those, SDSS J114657.79+403708.6 has the largest black hole mass, setting interesting constraints on the mass function of heavy ( $> 10^9 M_\odot$ ) black holes at high redshifts.

**Key words:** galaxies: active – quasars: general; quasars: supermassive black holes – X–rays: general

## 1 INTRODUCTION

Since the radiation produced by relativistic jets is strongly boosted along the jet direction, objects whose jet is pointing at us are very bright, and can be seen up to high redshifts. The black hole at the center of the powerhouse of these sources can be very massive, sometimes exceeding  $M = 10^{10} M_\odot$  (Ghisellini et al. 2009; 2010a). Therefore the hunt for high redshift blazars is an important field of research, allowing the census of heavy black holes in the early Universe. This can confirm or challenge existing theories of black hole formation, and even more so if we associate the presence of relativistic jets with a large black hole spin. In this case, in fact, the efficiency of accretion  $\eta$  (the fraction of accreted mass transformed into radiation) is higher than for a non–rotating black hole, reaching a value of  $\eta = 0.3$  for maximally rotating *accreting* black holes (see Thorne 1974). This implies that the Eddington luminosity is reached with a smaller accretion rate than for a non–rotating black hole. If the system is Eddington limited, this in turn implies a slower black hole growth. If a black hole seed starts to accrete at a redshift  $z = 20$  at the Eddington rate maintaining a large spin, it can reach a billion solar masses only at  $z < 4$  even for a seed mass as large as  $10^6 M_\odot$  (see e.g. Ghisellini et al. 2013). The very fact of the existence of radio–loud sources with  $M > 10^9 M_\odot$  at  $z > 4$  is thus a problem.

These issues motivate our search of high redshift blazars, keeping in mind that for each blazar (i.e. viewing angle smaller

than  $1/\Gamma$ , where  $\Gamma$  is the jet bulk Lorentz factor) there must be other  $2\Gamma^2$  sources whose jets are pointing in other directions.

Up to now there are two blazars known at  $z > 5$ : Q0906+6930 ( $z = 5.47$ , Romani et al. 2004; Romani 2006), and B2 1023+25 ( $z = 5.3$ , Sbarrato et al. 2012, 2013). The spectral energy distribution (SED) of these sources reveals both the thermal (i.e. strong optical emission lines and continuum) and the boosted non–thermal components. As in the majority of very powerful and high– $z$  blazars, the thermal disk emission becomes visible since it stands between the two non–thermal humps (the synchrotron one peaking in the sub–mm, and the high energy in the  $\sim$ MeV band; Ghisellini et al. 2010a; 2010b). In these sources the X–ray spectrum is hard [i.e.  $\alpha_X \sim 0.5$ , assuming  $F(\nu) \propto \nu^{-\alpha_X}$ ], and this, together with a relatively strong X–ray to optical flux ratio, can be taken as a signature of the blazar nature of the source.

In this letter we suggest that SDSS J114657.79+403708.6, a radio–loud AGN at  $z = 5.005$ , is a blazar, i.e. the viewing angle is smaller than  $1/\Gamma$ . Evidences for its blazar nature include its relatively large radio–loudness and its very large X–ray luminosity and hard X–ray spectrum, as measured by a pointed *Swift* observation. Infrared data collected by the WISE satellite (Wright et al. 2010), together with the Sloan Digital Sky Survey (SDSS; York et al. 2000) spectrum allowed to constrain the properties of the thermal emission.

In this work, we adopt a flat cosmology with  $H_0 = 70 \text{ km s}^{-1} \text{ Mpc}^{-1}$  and  $\Omega_M = 0.3$ .

\* E–mail: gabriele.ghisellini@brera.inaf.it

## 2 SDSS J114657.79+403708.6 AS A BLAZAR CANDIDATE

SDSS J114657.79+403708.6 (SDSS 1146+403 hereafter) belongs to the SDSS DR7 Quasar catalog (Schneider et al. 2010), that have been analysed by Shen et al. (2011). This sample contains  $\sim 105,000$  quasars. The area of the sky surveyed by the SDSS has been almost completely sampled by the the FIRST (Faint Images of the Radio Sky at Twenty-cm; Becker, White & Helfand, 1995) survey, with a flux limit of 1 mJy at 1.4 GHz. The sky area covered by both surveys is  $\sim 8,800$  square degrees. SDSS 1146+403 is detected in the radio with a flux of  $\sim 13$  mJy at 1.4 GHz, while VLBI observations yielded a flux of  $15.5 \pm 0.8$  and  $8.6 \pm 0.4$  mJy at 1.6 and 5 GHz, respectively (Frey et al. 2010). These fluxes correspond to a  $\nu L(\nu)$  radio luminosity of  $\sim 10^{44}$  erg s $^{-1}$ . Comparing the radio and the optical flux we obtain a radio loudness of  $\sim 100$ , calculated by assuming a flat radio spectrum (i.e.  $F(\nu) \propto \nu^0$ ) and calculating the rest frame 2500 Å flux (which is not observed) by extrapolating the continuum to  $\lambda = 1350$  Å.

SDSS 1146+403 is included in the AllWISE Source Catalog<sup>1</sup>, with clear detections in the two bands at lower wavelengths of the instrument, i.e.  $\lambda = 3.4 \mu\text{m}$  and  $\lambda = 4.6 \mu\text{m}$ . The source is not detected by the Large Area Telescope (LAT) onboard the *Fermi* satellite.

### 2.1 *Swift* observations

The large radio loudness of SDSS 1146+403 suggests a small viewing angle, and to confirm its blazar nature we observed the source with the *Swift* satellite (Gehrels et al. 2004). In fact the X–ray spectrum of FSRQs beamed towards us is particularly bright and hard, with an energy spectral index  $\alpha_x \sim 0.5$  [ $F(\nu) \propto \nu^{-\alpha_x}$ ] (see e.g. Ghisellini et al. 2010b, Wu et al. 2013).

The observations were performed between Jan. 16 and Jan 30 2013 (ObsIDs: 00049384001, 00049384002, 00049384003, 00049384004, 00049384005, 00049384007, 00049384008, 00049384009.). The ObsID 00049384001 e 00049384009 did not generate spectra nor light–curves.

Data of the X–ray Telescope (XRT, Burrows et al. 2005) and the UltraViolet Optical Telescope (UVOT, Roming et al. 2005) were downloaded from HEASARC public archive, processed with the specific *Swift* software included in the package HEASOFT v. 6.15 and analysed. The calibration database was updated on 12, 2013. We did not consider the data of the Burst Alert Telescope (BAT, Barthelmy et al. 2005), given the weak X–ray flux.

The total exposure on the XRT was  $\sim 40.8$  ks. The mean count rate was  $(1.74 \pm 0.21) \times 10^{-3}$ , resulting in 71 total counts. Given the low statistics, the fit with a power law model with Galactic absorption ( $N_{\text{H}} = 1.65 \times 10^{20}$  cm $^{-2}$ , Kalberla et al. 2005) was done by using the likelihood (Cash 1979). The output parameters of the model were a photon spectral index  $\Gamma_x = (\alpha_x + 1) = 1.5 \pm 0.3$  and an integrated observed flux  $F_{0.3-10 \text{ keV}} = (1. \pm 0.12) \times 10^{-13}$  erg cm $^{-2}$  s $^{-1}$ . The value of the likelihood was 54.93 for 63 dof. The X–ray data displayed in the SED (Fig. 2) has been rebinned to have  $3\sigma$  in each bin.

UVOT observed the source only in the *v* filter. The total was 61.2 ks. The source was not detected, and can derive a  $3\sigma$  upper limit  $v > 22.46$  mag. We expect, along the line of sight, some absorption due to the intervening matter. A rough estimate of the optical depth for the UVOT *v* filter for  $z = 5$  gives  $\tau \sim 2$  (F.

Haardt, priv. comm., see also Ghisellini et al. 2010a). Using this value of  $\tau$ , the unabsorbed upper limit on the flux in the *v* filter becomes  $F < 0.03$  mJy.

### 2.2 Estimate of the disc luminosity

We can infer the disc luminosity  $L_{\text{d}}$  in two ways. The first is by assuming that the IR–optical flux is due to accretion. The *WISE* IR data together with the optical spectrum redward of the Ly $\alpha$  SDSS 1146+403 provide a set of IR–optical data that show a rising (in  $\nu L_{\nu}$ ) slope and a peak around  $\sim 2 \times 10^{15}$  Hz (rest frame), below the absorption caused by intervening clouds (see Fig. 1). The  $\nu L_{\nu}$  luminosity at this peak is  $\sim 5 \times 10^{46}$  erg s $^{-1}$ , corresponding to an integrated IR–optical luminosity of  $10^{47}$  erg s $^{-1}$ . We associate this emission to the accretion disk. We can then immediately find the accretion rate assuming the accretion efficiency.

The second method relies on the presence of broad emission lines, that re–emit a fraction  $C$  (i.e. their covering factor) of the ionizing luminosity, assuming that the latter is provided by the accretion disc. The average value of  $C$  is around 0.1 (Baldwin & Netzer, 1978; Smith et al., 1981), with a rather large dispersion. This method, discussed in detail in Calderone et al. (2013), is based on templates of line to bolometric luminosities ratios, as the ones presented in Francis et al. (1991) or Vanden Berk et al. (2001). For instance in Francis et al. (1991) the ratio of the total luminosity of the broad line region (BLR hereafter) to the Ly $\alpha$  line luminosity is 5.5, while in van der Berk (2001) is 2.7. The SDSS optical spectrum of 1146+403 shows a prominent Ly $\alpha$ +NV line complex, which is absorbed in its blue part. Doubling the luminosity of only the red part, we obtain  $L_{L\text{Ly}\alpha} \sim 3 \times 10^{45}$  erg s $^{-1}$ . This corresponds to  $L_{\text{BLR}} = (0.8-1.7) \times 10^{46}$  erg s $^{-1}$ . If  $C = 0.1$ , the disk luminosity is then 10 times greater. Within the relevant uncertainties, the agreement between the two methods is rather satisfactory.

### 2.3 Estimate of the black hole mass

A robust lower limit to the black hole mass of SDSS 1146+403 is set by assuming that its disc emits at the Eddington luminosity. This implies  $M > 10^9 M_{\odot}$ .

The commonly used virial method, based on the relation between the ionizing luminosity and the distance of the BLR, and on the assumption that the velocity of the clouds is virialized and it is linked to gravity (e.g. Wandel 1997; Peterson et al. 2004) is not (yet) applicable in this case, because we do not have the appropriate scaling relations for the Ly $\alpha$  line (which in addition has an uncertain FWHM, since its blue wing is absorbed) and we do not have (yet) an IR spectrum of the source that can reveal the CIV and the MgII broad lines.

We then apply the method of fitting a disk accretion model spectrum to the data. We assume a simple Shakura & Sunyaev disk (1973) model, which depends only on the black hole mass  $M_{\text{BH}}$  and on the accretion rate  $\dot{M}$ . The latter is traced by the total disc luminosity  $L_{\text{d}} = \eta \dot{M} c^2$ . For simplicity, we assume that the black hole is non rotating and set  $\eta = 0.08$  and the last stable orbit at 3 Schwarzschild radii. If we measure  $L_{\text{d}}$  (hence  $\dot{M}$ ), we are left with  $M_{\text{BH}}$  as the only remaining free parameter. For a given  $\dot{M}$ , the black hole mass determines the peak frequency of the disc emission. A larger mass implies a larger disc surface and hence a lower temperature emitting a given luminosity. Therefore, for a fixed  $L_{\text{d}}$ , a larger  $M_{\text{BH}}$  shifts the peak to lower frequencies. Then the best agreement with the data fixes  $M_{\text{BH}}$  (e.g. Calderone et al. 2013).

<sup>1</sup> Data retrieved from <http://irsa.ipac.caltech.edu/>

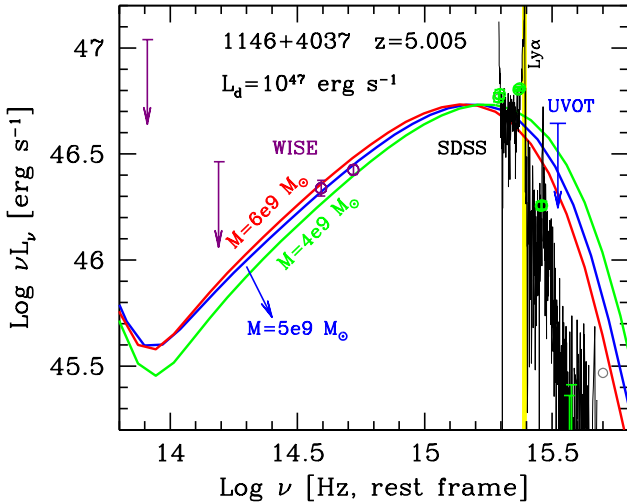


**Figure 1.** Optical–UV SED of SDSS 1146+403 in the rest frame, together with models of standard accretion disc emission. Optical and UV data, including the SDSS spectrum, have been corrected for the extinction in our Galaxy. Data from WISE (AllWISE Source Catalog) and GROND, and the SDSS spectrum are labelled. Green points are archival data taken from ASDC SED builder. The two optical photometric points receive some contribution from the emission line flux, besides the continuum. We show the spectrum of three accretion disc models with the same luminosity and different  $M_{\text{BH}}$ :  $M_{\text{BH}}/M_{\odot} = 6 \times 10^9$  (red),  $5 \times 10^9$  (blue) and  $4 \times 10^9$  (green). Note that outside this range of masses, the model cannot fit satisfactory the data.

Using a larger efficiency would enhance the emission at high (rest frame UV) frequencies. Assuming that the disk emits the same  $L_d$ , this implies a smaller flux below the disk emission peak. To match the optical–IR emission one would then require a larger black hole mass (see the discussion on this issue in Calderone et al. 2013).

Fig. 1 shows the data in the IR–optical band (as labelled) and three disc emission spectra calculated assuming the same  $L_d$  and three different mass values:  $M_{\text{BH}} = 6 \times 10^9 M_{\odot}$  (red line),  $5 \times 10^9 M_{\odot}$  (blue) and  $4 \times 10^9 M_{\odot}$  (green). These values are indicative of the uncertainties on the black hole mass, which is therefore  $(5 \pm 1) \times 10^9 M_{\odot}$ .

### 3 OVERALL SPECTRAL ENERGY DISTRIBUTION

Fig. 2 shows the overall SED of SDSS 1146+403 from radio to  $\gamma$ -rays. The optical data and the SDSS spectrum have been corrected for galactic extinction. The dashed line in the radio domain indicates a flat radio spectrum  $F_{\nu} \propto \nu^0$ , while the grey hatched area corresponds to the limiting sensitivity of *Fermi*/LAT. The lower boundary is the  $5\sigma$  flux limit for 5 years of *Fermi* operations. The same figure shows the result of a fitting model, described in detail in Ghisellini & Tavecchio (2009). It is a one–zone, leptonic model, in which relativistic electrons emit by the synchrotron and Inverse Compton processes. The electron distribution is derived through a continuity equation, assuming continuous injection, radiative cooling, possible pair production and pair emission, and is calculated at a time  $R/c$  after the start of the injection, where  $R$  is the size of

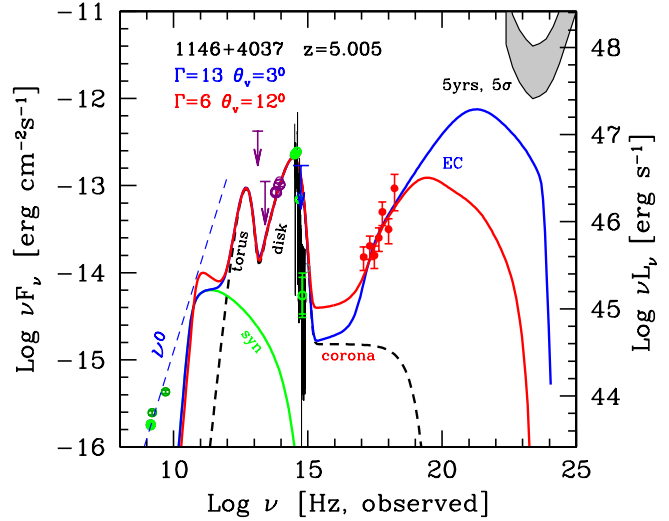


**Figure 2.** SED of SDSS 1146+403 together with the adopted models, as labelled. Data from WISE, GROND, *Swift*/XRT and *Fermi*/LAT are labelled. Green points are archival data taken from ASDC SED builder. The solid green line is the synchrotron component of the model, the dashed black line is the torus+disc+X–ray corona component. The high energy emission is dominated by the External Compton (EC) component. The lower bound of the grey stripe correspond to the LAT upper limits for 5 years,  $5\sigma$ .

the source, located at a distance  $R_{\text{diss}}$  from the black hole. The jet is viewed at an angle  $\theta_v$  from the jet axis. The accretion disk component is accounted for, as well the infrared emission reprocessed by a dusty torus and the X–ray emission produced by a hot thermal corona sandwiching the accretion disc. We present two models. The first ( $\Gamma = 13$ ;  $\theta_v = 3^\circ$ ) is the best representation of the data assuming a set of parameters very similar to other powerful blazars (Ghisellini et al., 2010a; 2010b), while the second assumes  $\Gamma = 6$  and  $\theta_v = 12^\circ$ . This latter choice corresponds to the model with the maximum viewing angle compatible with the data and a still reasonable bulk Lorentz factor. Tab. 1 reports the relevant parameters of the two models of SDSS 1146+403, together with the parameters for the other two blazars at  $z > 5$ .

Both models fit the X–radio data and are very similar in the radio band. Having the same black hole mass and accretion rate, they have the same shape and flux in the IR–optical range. However, they correspond to jets with a very different intrinsic power. The small  $\Gamma$ , relatively large  $\theta_v$  solution implies a much less beamed emission, and therefore demands a greater intrinsic power. This leads us to prefer the more “economic” solution. Note that the models differ in the hard X–ray range, where the source could be detected by the *NuSTAR* satellite (sensitive up to  $\sim 80$  keV; Harrison et al. 2013).

#### 3.1 Comparison with Q0906+6930 and B2 1023+25

Fig. 3 shows how the SED of 1146+403 compares with the SED (in  $\nu L_{\nu}$  vs rest frame  $\nu$ ) of Q0906+693 ( $z=5.47$ ) and B2 1023+25 ( $z=5.3$ ). As can be seen, the three SEDs are very similar. All three sources have approximately the same IR–optical spectrum, and also the X–ray spectra are remarkably similar. The main difference is in

Name	$z$	$R_{\text{diss}}$	$M$	$R_{\text{BLR}}$	$P'_i$	$L_d$	$L_d/L_{\text{Edd}}$	$B$	$\Gamma$	$\theta_v$	$\gamma_b$	$\gamma_{\text{max}}$	$P_r$	$P_B$	$P_e$	$P_p$
[1]	[2]	[3]	[4]	[5]	[6]	[7]	[8]	[9]	[10]	[11]	[12]	[13]	[14]	[15]	[16]	[17]
1146+430	5.005	900	5e9	1006	7e-3	100	0.15	1.4	13	3	230	3e3	3.7	10.3	0.05	15.1
1146+430	5.005	900	5e9	1006	0.8	100	0.15	1.5	6	12	50	3e3	75.9	2.3	4.6	741
0906+693	5.47	630	3e9	822	0.02	67.5	0.17	1.8	13	3	100	3e3	10.4	8.2	0.2	58
1023+25	5.3	504	2.8e9	920	0.01	90	0.25	2.3	13	3	70	4e3	5	8.5	0.14	40.7

**Table 1.** List of parameters adopted for or derived from the model for the ED of SDSS 1146+403, compared with the set of parameters used for the other two blazars at  $z > 5$ . Col. [1]: name; Col. [2]: redshift; Col. [3]: dissipation radius in units of  $10^{15}$  cm; Col. [4]: black hole mass in solar masses; Col. [5]: size of the BLR in units of  $10^{15}$  cm; Col. [6]: power injected in the blob calculated in the comoving frame, in units of  $10^{45}$  erg  $s^{-1}$ ; Col. [7]: accretion disk luminosity in units of  $10^{45}$  erg  $s^{-1}$ ; Col. [8]:  $L_d$  in units of  $L_{\text{Edd}}$ ; Col. [9]: magnetic field in Gauss; Col. [10]: bulk Lorentz factor at  $R_{\text{diss}}$ ; Col. [11]: viewing angle in degrees; Col. [12] and [13]: break and maximum random Lorentz factors of the injected electrons; Col. [14]: power spent by the jet to produce the non-thermal beamed radiation in units of  $10^{45}$  erg  $s^{-1}$ ; Col. [15]: jet Poynting flux in units of  $10^{45}$  erg  $s^{-1}$ ; Col. [16]: power in bulk motion of emitting electrons, in units of  $10^{45}$  erg  $s^{-1}$ . Col. [17]: power in bulk motion of cold protons, assuming one proton per emitting electron in units of  $10^{45}$  erg  $s^{-1}$ . The total X-ray corona luminosity is assumed to be in the range 10–30 per cent of  $L_d$ . Its spectral shape is assumed to be always  $\propto \nu^{-1} \exp(-h\nu/150 \text{ keV})$ .

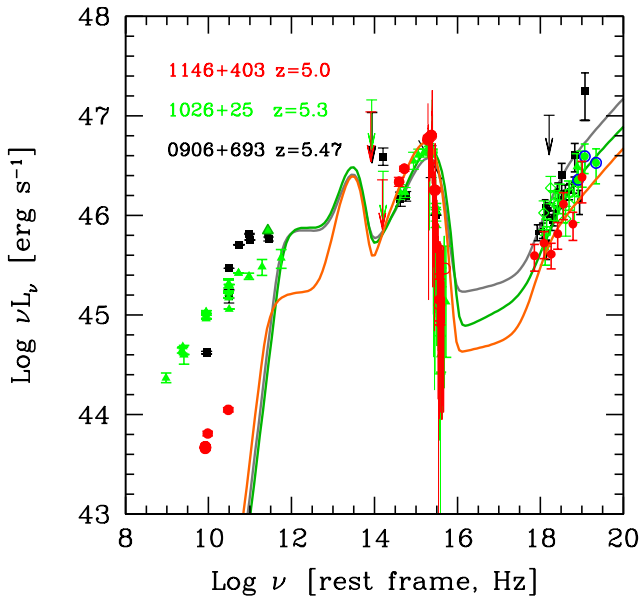


**Figure 3.** Comparison between the SED of SDSS 1146+403 (red symbols) with B2 1023+25 (green symbols) and Q0906+6930 (black symbols). The solid lines corresponds to the models whose parameters are listed in Tab. 1 (for 1146+403 we show the model with  $\Gamma = 13$  and  $\theta_v = 3^\circ$ ). The three sources are very similar in the IR–optical and X-rays, but SDSS 1146+403 is a factor  $\sim 20$  less luminous in the radio. The strong X-ray luminosity (with respect to the optical) and the hard X-ray spectra flag the presence of jet radiation beamed in the observer’s direction. The difference in the radio band could be due to a slight bend of the jet between the regions emitting X-rays (inner jet) and the radio (more external jet).

the radio band, with SDSS 1146+403 being under-luminous by a factor  $\sim 20$  with respect to the other two blazars.

The X-ray emission in blazars is usually produced in a rather compact region of the jet, possibly within the BLR. This is the most efficient way to produce high energy photons through inverse Compton scattering, due to the presence of emission line photons, besides the synchrotron photons produced internally to the jet. Furthermore, a compact region can account for the short time variability often shown by blazars. On the other hand, if the X-ray flux

is variable, the approximate equal X-ray flux detected in the three sources must be a coincidence. The lack of strong variability could be explained, in the adopted model, by the fact that the X-rays are produced by low energy electrons (with random Lorentz factors  $\gamma \lesssim 2-5$ ) scattering emission line photons: since the cooling time  $\propto 1/\gamma$ , these electrons may have not time to cool in one dynamical time  $R/c$ . Consequently, the X-ray flux they produce is less variable than at higher ( $\gamma$ -ray) energies, characterized by a much shorter cooling time.

The size of the region emitting the radio flux at  $\sim$  GHz frequencies must be much larger (and therefore more external) than the X-ray region, since otherwise the flux would be self-absorbed. This is the reason why our one-zone model cannot reproduce the radio below a several tens of GHz. The smaller radio flux of SDSS 1146+403 could then be due to a jet bending between the X-ray and the radio regions. Assuming a constant  $\Gamma = 13$ , the radio deficit (factor  $\sim 20$ ) can be explained by a change in viewing angle from  $\theta_v = 3^\circ$  (corresponding to the X-ray production region of the jet) to  $\theta_v = 6^\circ$  (corresponding to the jet region producing the radio).

Alternatively, the jet could decelerate between the two regions maintaining the same viewing angle: in this case  $\Gamma$  must decrease by a factor  $20^{1/4} \sim 2.1$ . However, in this case, the deceleration should correspond to a relevant dissipation, in turn corresponding to some emission, which we do not see. It would be interesting to observe the source at high radio frequencies (100–300 GHz, rest frame), to see if the radio deficit remains the same or becomes smaller.

## 4 DISCUSSION AND CONCLUSIONS

In this letter we propose that the radio-loud, high redshift quasar SDSS 1146+403 is a blazar. If so, it is the third most distant blazar known up to now, with redshift  $z = 5.005$ , that corresponds to a cosmic age 1.1 billion years. Despite this young age, the black hole of SDSS 1146+403 managed to grow to 5 billion solar masses.

Both its thermal and non-thermal components are very luminous. In agreement with the blazar sequence (Fossati et al. 1998) the two broad non-thermal humps peak at small frequency. In particular, the hard X-ray spectrum and the upper limit in the  $\gamma$ -ray band constrain the high energy component to peak in the MeV region of the spectrum. Therefore this source, along with the similar other powerful blazars, should have a relatively large hard X-ray

flux and would have been an ideal target for hard X-ray instruments such as the focussing hard X-ray telescope *NuStar* (Harrison et al., 2013). The great sensitivity over its energy range [5–80 keV] would enable it to detect the hard X-ray spectrum of this source, even if it cannot directly observe the peak of the high energy hump.

It is possible to roughly estimate the number of these objects and their spatial density.

The comoving density of heavy black holes at high redshifts of radio-loud sources has been studied by Volonteri et al. (2011), based on the 3 years BAT catalog and the blazar luminosity function, in hard X-rays, derived by Ajello et al. (2009), and modified (beyond  $z = 4.3$ ) by Ghisellini et al. (2010a). In the latter paper the observational constrain on the blazar density with black holes heavier than  $10^9 M_\odot$  in the redshift bin  $5 < z < 6$  was based on the detection of only one object: Q0906+6930. Assuming it was the only blazar in the entire sky in this redshift bin, Ghisellini et al. (2010a) derived a comoving density of  $2.63 \times 10^{-3} \text{ Gpc}^{-3}$  of blazars hosting an heavy black hole in the  $5 < z < 6$  bin (see Fig. 15 in that paper).

SDSS 1146+403 was selected in the SDSS catalog covered by FIRST observations, and the common area of the sky of these two surveys is 8770 square degrees. It is the second source that can be classified as a blazars in this SDSS+FIRST survey (together with B2 1023+25). The comoving volume in the redshift bin  $5 < z < 6$  is  $380 \text{ Gpc}^3$ . Therefore the number density of blazars in this redshift bin is  $N_{BL} = 2 \times (40,000/8,770)/380 = 2.4 \times 10^{-2} \text{ Gpc}^{-3}$ . Both B2 1023+25 and SDSS 1146+403 have black holes with  $M > 10^9 M_\odot$ . To find out the density of black holes in jetted sources heavier than one billion solar masses, we should consider that for each jet observed within a viewing angle  $\theta_v = 1/\Gamma$ , there exist another  $2\Gamma^2$  sources pointing in other directions. So the number density of black holes with  $5 < z < 6$ , with a mass exceeding  $10^9 M_\odot$ , is  $0.024 \times 2 \times 169(\Gamma/13)^2 = 8.1 \text{ Gpc}^{-3}$ . Multiplying by the comoving volume gives  $\sim 3,000$  heavy black holes in jetted sources only.

As mentioned in the introduction, the finding of heavy and early black holes in sources with jets can severely challenge our understanding of black hole growth, especially if we associate the presence of the jet with a rapidly spinning black hole. A Kerr black hole is in fact more efficient to transform gravitational energy into radiation than a non spinning (radio-quiet) black hole. This lends support to the possibility of super-Eddington accretion (Volonteri & Silk 2014), and/or to the possibility that part of the gravitational energy of the accreting matter is not used to heat the disk, but to amplify the magnetic fields necessary to extract the rotational energy of the black hole (see e.g. Jolley & Kunzic 2008; Shankar et al. 2008, Ghisellini et al. 2013 ).

## ACKNOWLEDGEMENTS

We thank the anonymous referee for useful comments. This publication makes use of data products from the Wide-field Infrared Survey Explorer, which is a joint project of the University of California, Los Angeles, and the Jet Propulsion Laboratory/California Institute of Technology, funded by NASA. Part of this work is based on archival data and on-line service provided by the ASI Science Data Center (ASDC).

## REFERENCES

- Baldwin J.A. & Netzer H., 1978, ApJ, 226, 1  
 Barthelmy S., Barbier L., Cummings J. et al., 2005, Space Sci. Rev. 120, 143  
 Becker R.H., White R.L., & Helfand D.J. 1995, ApJ, 450, 559  
 Burrows D., Hill J., Nousek J., et al., 2005, Space Sci. Rev. 120, 165  
 Calderone G., Ghisellini G., Colpi M. & Dotti, M., 2013, MNRAS, 431, 210  
 Cash W., 1979, ApJ, 228, 939  
 Fossati G., Maraschi L., Celotti A., Comastri A. & Ghisellini G., 1998, MNRAS, 299, 433  
 Francis P.J., Hewett P.C., Foltz C.B., Chaffee F.H., Weymann R.J. & Morris S.L., 1991, ApJ, 373, 465  
 Frey S., Paragi Z., Gurvits L.I., Cseh D. & Gabanyi K.E., 2010, A&A, 524, A83  
 Gehrels N., Chincarini G., Giommi P. et al., 2004, ApJ, 611, 1005  
 Ghisellini G., Foschini L., Volonteri M., Ghirlanda G., Haardt F., Burlon D. & Tavecchio F., 2009, MNRAS, 399, L24  
 Ghisellini G. & Tavecchio F., 2009, MNRAS, 397, 985  
 Ghisellini G., Della Ceca R., Volonteri M. et al., 2010a, MNRAS, 405, 387  
 Ghisellini G., Tavecchio F., Foschini L., Ghirlanda G., Maraschi L. & Celotti A., 2010b, MNRAS, 402, 497  
 Ghisellini G., Haardt F., Della Ceca R., Volonteri M. & Sbarrato T. 2013, MNRAS, 428, 1449  
 Harrison, F.A. William W. Craig W.W., Christensen F.E., 2013, ApJ, 770, 103  
 Jolley E.J.D & Kuncic Z., 2008, MNRAS, 386, 989  
 Kalberla P.M.W., Burton W.B., Hartmann D., Arnal E.M., Bajaja E., Morras R. & Pöppel W.G., 2005, A&A, 440, 775  
 Peterson B.M., Ferrarese L., Gilbert K.M. et al., 2004, ApJ, 613, 682  
 Romani R.W., Sowards-Emmerd D., Greenhill L. & Michelson P., 2004, ApJ, 610, L9  
 Romani R.W., 2006, AJ, 132, 1959  
 Roming P., Kennedy T., Mason K. et al., 2005, Space Sci. Rev. 120, 95  
 Sbarrato T., Ghisellini G., Nardini M., et al., 2012, MNRAS, 426, L91  
 Sbarrato T., Tagliaferri G., Ghisellini G. et al., 2013, ApJ, 777, 147  
 Schneider D. P., Richards, G. T., Hall P. B. et al., 2010, AJ, 139, 2360S  
 Shakura N.I. & Sunjaev R.A., 1973, A&A, 24, 337  
 Shankar F., Cavaliere A., Cirasuolo M. & Maraschi L., 2008, ApJ, 676, 131  
 Shen Y., Richards G.T., Strauss M.A. et al., 2011, ApJS, 194, 45  
 Smith M.G., Carswell R.F., Whelan J.A.J et al., 1981, MNRAS, 195, 437  
 Thorne K.S., 1974, ApJ, 191, 507  
 Vanden Berk D.E., Richards G.T., Bauer A. et al., 2001, AJ, 122, 549  
 Volonteri M., Haardt F., Ghisellini G. & Della Ceca R., 2011, MNRAS, 416, 216  
 Volonteri M. & Silk J., 2013, *submit to ApJL (astro-ph/1401.3513)*  
 Wandel A., 1997, ApJ, 490, L131  
 Wright E.L., Eisenhardt P.R.M., Mainzer A.K. et al., 2010, AJ, 140, 1868  
 Wu J., Brandt W. N., Miller B.P., Garmire G.P., Schneider D.P., Vignali C., 2013, ApJ, 763, 109  
 York D.G., Adelman J., Anderson J.E. et al., 2000, AJ, 120, 1579